# A New Look at Calibration and Use of Eppley Precision Infrared Radiometers. Part I: Theory and Application

C. W. FAIRALL

*NOAA/ERL/Environmental Technology Laboratory, Boulder, Colorado*

P. O. G. PERSSON

*Cooperative Institute for Research in Environmental Sciences, University of Colorado/NOAA, Environmental Technology Laboratory, Boulder, Colorado*

E. F. BRADLEY

*CSIRO Centre for Environmental Mechanics, Canberra, Australia*

R. E. PAYNE AND S. P. ANDERSON

*Woods Hole Oceanographic Institution, Woods Hole, Massachusetts*

(Manuscript received 28 July 1997, in final form 26 December 1997)

ABSTRACT

The calibration and accuracy of the Eppley precision infrared radiometer (PIR) is examined both theoretically and experimentally. A rederivation of the fundamental energy balance of the PIR indicates that the calibration equation in common use in the geophysical community today contains an erroneous factor of the emissivity of the thermopile. If a realistic value (0.98) for the emissivity is used, then this leads to errors in the total flux of 5–10 W $m^{-2}$. The basic precision of the instrument is found to be about 1.5% of the total IR irradiance when the thermopile voltage and both dome and case temperatures are measured. If the manufacturer's optional battery-compensated output is used exclusively, then the uncertainties increase to about 5% of the total (20 W $m^{-2}$). It is suggested that a modern radiative transfer model combined with radiosonde profiles can be used as a secondary standard to improve the absolute accuracy of PIR data from field programs. Downwelling IR fluxes calculated using the Rapid Radiative Transfer Model (RRTM), from 55 radiosondes ascents in cloud-free conditions during the Tropical Oceans Global Atmosphere Coupled Ocean–Atmosphere Response Experiment field program, gave mean agreement within 2 W $m^{-2}$ of those measured with a shipborne PIR. PIR data from two sets of instrument intercomparisons were used to demonstrate ways of detecting inconsistencies in thermopile-sensitivity coefficients and dome-heating correction coefficients. These comparisons indicated that pairs of PIRs are easily corrected to yield mean differences of 1 W $m^{-2}$ and rms differences of 2 W $m^{-2}$. Data from a previous field program over the ocean indicate that pairs of PIRs can be used to deduce the true surface skin temperature to an accuracy of a few tenths of a kelvin.

## 1. Introduction

Atmospheric radiative fluxes represent a critical component of atmospheric dynamics, climate, boundary layer physics, and air–surface interactions. Advances in radiative transfer models and continued improvements in the technology of atmospheric turbulent fluxes are placing increasing demands for improvements in radiative flux methods and instruments. For example, the recent Tropical Oceans Global Atmosphere (TOGA) Coupled Ocean–Atmosphere Response Experiment (COARE) set a goal of $\pm 10$ W $m^{-2}$ uncertainty for determinations of the total surface heat input to the ocean mixed layer (Webster and Lukas 1992). The COARE Flux Working Group (Bradley and Weller 1993; Fairall et al. 1996a) suggested that an accuracy of each of the principal flux components (net solar flux, net IR flux, and sum of the sensible and latent turbulent heat fluxes) of $\pm 6$–7 W $m^{-2}$ was required. To meet this goal, it is necessary to measure downward IR flux from ships and buoys to an accuracy of about $\pm 5$ W $m^{-2}$. The steps taken to accomplish this goal are described by Bradley et al. (1996, manuscript submitted to *J. Atmos. Oceanic Technol.*). One of these steps was an examination of radiative flux measurements that is described in detail in the present paper.

*Corresponding author address:* C. W. Fairall, NOAA/ERL/Environmental Technology Laboratory, R/E/ET7, 325 Broadway, Boulder, CO 80303-3328.
E-mail: cfairall@etl.noaa.gov

The pyrgeometer is an instrument frequently used for performing hemispherical, broadband, IR radiative flux measurements. Commercial instruments have been available from several manufacturers in the United States, Japan, and Europe for decades. These instruments consist of a black-painted thermopile with one junction set in contact with a temperature reservoir in the form of a heavy metal base, and the other junction set radiatively exposed to the atmosphere through a filter dome that rejects radiation in the solar band and insulates the thermopile from direct heat transfer by the air. Surface-based measurement of downward IR flux with such instruments involves consideration of platform motion and/or vertical alignment (Katsaros and DeVault 1986; MacWhorter and Weller 1991), the contaminating effects of solar radiation heating the dome (Albrecht et al. 1974; Enz et al. 1975; Alados-Arboledas et al. 1988), the calibration of the instruments (Weiss 1981; Eppley Laboratory, Inc. 1995; Philipona et al. 1995), and the basic equation describing the radiometer performance (Albrecht et al. 1974; Albrecht and Cox 1977; Alados-Arboledas et al. 1988).

Scientific opinion regarding the fundamental accuracy of the pyrgeometer varies considerably. The authors of this paper have heard informal statements about absolute pyrgeometer accuracy made by numerous practitioners of the field; their estimates run the gamut from 5% to 5 W $m^{-2}$. Albrecht et al. (1974) stated that, provided dome and case temperature effects are determined accurately, the pyrgeometer ''may be used to measure infrared irradiance with a precision of $\pm 2$ W $m^{-2}$.'' Similar claims are made by Philipona et al. (1995). Instruments manufactured by Eppley Laboratory, Inc. (1976) are specified to be linear to 1%, temperature-corrected to 2%, and have a cosine response to 5% accuracy. Accuracy of the factory determinations of the voltage-to-flux sensitivity coefficient is not stated, but successive calibrations typically change by about 3%. These statistics suggest that the 5% uncertainty is more representative of the truth. A 5% uncertainty for a 400 W $m^{-2}$ downward IR flux is an uncertainty of 20 W $m^{-2}$; this is clearly not within the COARE goal.

Why is the accuracy of the pyrgeometer so uncertain? The authors of this paper have participated in nearly 200 meteorological and oceanographic research field programs in the last 35 years. It is our experience that pyrgeometers are used by a variety of geophysical investigators with little interest in the fine points of radiative transfer theory and the elegance of modern radiometers; rather, they are pursuing interests in meteorology and oceanography for which the radiative flux is but one of a number of energy components that they must account for to get at their science. We have observed that these investigators use different data-acquisition approaches and even different equations to compute the radiative flux from the same basic measurements. For example, the Eppley Laboratory, Inc., precision infrared radiometer (PIR) comes with a battery-powered resistance network that provides a voltage that expresses the radiative flux contribution of the temperature reservoir. It also has terminals connected to the case thermistor that allow the user to measure the case (reservoir) temperature and directly compute this component. This computation may or may not account for the emissivity of the paint used on the thermopile. This emissivity is about 0.98, but in the literature, and even in Eppley's documentation, the emissivity may be approximated by 1.0. Eppley also provides the option of attaching a thermistor to the radiometer dome for monitoring of the dome temperature. Thus, one may connect as few as two wires to an Eppley PIR or as many as six wires and process the raw data with a choice of several different equations.

In the authors' opinion, this bewildering variety of options has led to confusion about the performance of conventional pyrgeometers and numerous incidences in which radiometers were used in a manner that significantly increased the errors. For example, the COARE experiment involved measurements of downward IR flux from six research ships and one buoy, yet only one of these platforms logged the pyrgeometer thermopile output along with both the case and dome temperatures. In a recent planning meeting for the Surface Heat Budget of the Arctic (SHEBA) program, three of seven groups planning to employ pyrgeometers were unaware that use of the battery output compromised the measurement accuracy.

The purpose of this paper is to clear up this confusion to allow nonexperts to make better measurements with commercial instruments using factory calibrations. In the present paper, we will restrict our analysis to the PIR manufactured by Eppley Laboratory because this instrument represents the vast majority of our experience, and its operation and calibration is well documented (Eppley Laboratory, Inc., 1976, 1994, 1995). A companion paper (Payne and Anderson 1999, hereafter Part II) describes an more robust and complex alternative to the Eppley factory calibration method. The basic principles of our developments will apply to similar instruments from other manufacturers, but specific details may not apply. In section 2 we will reexamine the fundamental heat balance equation of the pyrgeometer and its relationship to the sensitivity and dome temperature correction effect. In section 3 we examine the official Eppley calibration procedure and establish its relationship to our fundamental equation. In section 4 we provide a detailed error analysis of the PIR and discuss the relative accuracy of different acquisition modes and uncertainties associated with different calibration equations. In section 5 we validate the fundamental PIR equation using instrument and model intercomparisons. In section 6 conclusions are given.

## 2. The pyrgeometer energy balance equation

Albrecht et al. (1974) performed an analysis of the energy balance of the pyrgeometer, which we summarize

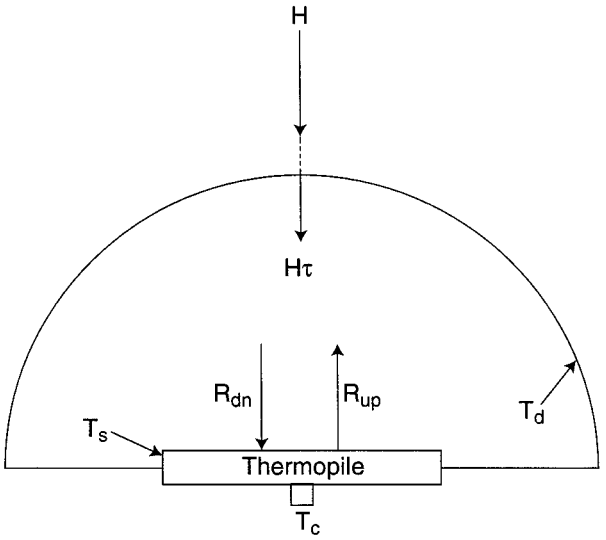


FIG. 1. Diagram of flux balance of the PIR thermopile and dome. Here $H$ is the downward ambient longwave irradiance; $\tau$ is the transmission coefficient of the dome. The dome is at temperature $T_d$, the case is at temperature $T_c$, and the top of the thermopile is at temperature $T_s$. The downward and upward longwave irradiances at the surface of the thermopile are $R_{dn}$ and $R_{up}$.

here. Figure 1 shows a diagram of the various energy fluxes. The output of the thermopile $\Delta V$ is a voltage proportional to the temperature difference between the top and bottom of the thermopile $\Delta T$. The bottom of the thermopile is in thermal contact with the pyrgeometer case at temperature $T_c$, while the upper surface radiates with a characteristic surface temperature, $T_s$. This temperature difference is maintained by thermal conduction through the thermopile; the conductive process transfers heat from the case to balance the net radiative loss from the top of the thermopile:

$$\text{Flux} = R_{\text{net}} = R_{\text{dn}} - R_{\text{up}} = k\Delta T, \tag{1}$$

where $k$ is the thermal conductivity of the thermopile, $R_{\text{dn}}$ the downward IR flux, $R_{\text{up}}$ the upward IR flux just above the thermopile, and $\Delta T = T_s - T_c$. Albrecht et al. (1974) wrote the individual radiative flux terms as

$$R_{\text{up}} = \epsilon_o \sigma T_s^4 \tag{2a}$$

$$R_{\text{dn}} = H\tau + \epsilon_o \rho \sigma T_s^4 + \epsilon \sigma T_d^4, \tag{2b}$$

where $\sigma$ is the Stefan–Boltzmann constant; $\tau$, $\rho$, and $\epsilon$ are the IR transmission, reflection, and absorption (emission) coefficients for the pyrgeometer dome, respectively; $T_d$ is the dome temperature; and $H$ is the downward IR flux from the atmosphere (i.e., the quantity we are attempting to measure). Here, $\epsilon_o$ is the emissivity of the paint (Parsons' Black for the Eppley PIR) on the thermopile. The single term on the right side of (2a) represents the flux emitted by the thermopile; the first term on the right side of (2b) is the flux transmitted by the dome, the second is the upward flux from the thermopile that is reflected back by the dome, and the third is the flux emitted downward by the dome.

These equations are solved to yield the incident flux

$$H\tau = k\Delta T + \epsilon_o \sigma T_s^4 - \epsilon_o \rho \sigma T_s^4 - \epsilon \sigma T_d^4. \tag{3}$$

After rearranging, Albrecht et al. (1974) substituted the normal relation $\rho = 1 - \tau - \epsilon$ and then wrote (3) as

$$H\tau = k\Delta T + \epsilon_o \tau \sigma T_s^4 + \epsilon \sigma(\epsilon_o T_s^4 - T_d^4). \tag{4}$$

Albrecht et al. (1974) substituted $T_s = T_c + \Delta T$ and expanded to first order to obtain

$$H = [k/\tau + 4(1 + \epsilon/\tau)\epsilon_o \sigma T_c^3]\Delta T + \epsilon_o \sigma T_c^4 + (\epsilon/\tau)\sigma(T_c^4 - T_d^4), \tag{5}$$

where $\epsilon_o$ is set to 1 in the last term on the right. The relationship between the thermopile temperature difference and its voltage output $\Delta V$ is well known (Fritschen and Gay 1979):

$$\Delta T = \alpha \Delta V, \tag{6}$$

where $\alpha \approx 694$ K V$^{-1}$ (Eppley Laboratory, Inc. 1995). Therefore, we arrive at the Albrecht et al. (1974) radiometer calibration equation:

$$H = \Delta V/s + \epsilon_o \sigma T_c^4 + B\sigma(T_c^4 - T_d^4). \tag{7}$$

Here, $s$ is the radiometer sensitivity factor

$$s^{-1} = [k/\tau + 4\epsilon_o \sigma T_c^3(1 + \epsilon/\tau)]\alpha, \tag{8}$$

which is usually quoted in $\mu$V/(W m$^{-2}$) and $B = \epsilon/\tau$.

Albrecht et al. (1974) referred to the $s$ term as the "temperature-compensated thermopile output." However, it is important to realize that for Eppley instruments the thermopile temperature compensation is supplied so that the factor $\alpha$ is approximately independent of temperature ($\pm 2\%$); temperature dependence associated with the $T_c^3$ still remains. They also point out that Eppley pyrgeometers are supplied with a battery-compensated output that is added to the thermopile voltage so that only one voltage measurement is required. We will return to this issue later. Also, (7) is the form of the pyrgeometer equation supplied by Eppley for those requesting instruments with both case and dome temperature sensors; $\epsilon_o$ is quoted as having a value of 0.98 or 0.985 for the Parsons' Black paint used on the thermopile. The Albrecht et al. (1974) formulation is commonly referenced when PIR measurements are described, although $\epsilon_o$ may be set to 0.98 (e.g., Weiss 1981; Fairall et al. 1990; Ruffieux et al. 1995), assumed to be 1.0 (e.g., Albrecht and Cox 1977; Olivieri 1991; Philipona et al. 1995), does not appear at all (e.g., Miskolczi 1994; Miskolczi et al. 1997), or the value used may not be stated (e.g., Dutton 1993). In none of the papers where $\epsilon_o$ is assumed to be 1.0, or where it is left out, is it clearly stated that a factor of $\epsilon_o$ should not be multiplying $\sigma T_c^4$.

The primary problem with the Albrecht et al. (1974) development is that both (2a) and (2b) apply the $\epsilon_o \approx$

1 approximation inconsistently, $(1 - \epsilon_o) = \rho_o$ is set to zero, but $\epsilon_o$ is not set to 1.0. The correct forms of these equations are

$$R_{\text{up}} = \epsilon_o \sigma T_s^4 + \rho_o R_{\text{dn}} \tag{9a}$$

and

$$R_{\text{dn}} = H\tau + \epsilon\sigma T_d^4 + \rho R_{\text{up}}. \tag{9b}$$

The second term in (9a) is necessary to establish the correct upward radiative flux; this form is recognizable as the normal expression for the upward part of the surface energy balance. In (9b) the reflection of the surface emission term from (2b) must be replaced by the entire upward flux. These equations are easily solved as before:

$$H\tau = k\Delta T[1 - (1 - \epsilon_o)\rho]/\epsilon_o + \tau\sigma T_s^4 + \epsilon\sigma(T_s^4 - T_d^4). \tag{10}$$

We now arrive at what we will define as the fundamental radiometer calibration equation,

$$H = \Delta V/s_o + \sigma T_s^4 + B\sigma(T_s^4 - T_d^4), \tag{11}$$

where the factor $B$ is the same as in (7). Here, $s_o$ is termed the fundamental radiometer sensitivity constant

$$s_o^{-1} = k[1 - (1 - \epsilon_o)\rho]\alpha/(\epsilon_o\tau) \tag{12}$$

because it contains no explicit temperature dependence. The calibration factors $s_o$ and $B$ are usually determined by direct calibration rather than computation from values for $\epsilon$, $\rho$, $\tau$, $k$, and $\alpha$. If we assume that $\rho$ is small, then a typical value of $B = 3.5$ implies $\tau \approx 0.22$, which explains why the sensitivity coefficient of the silicon-domed pyrgeometer is less than half that of the Eppley pyranometer (which uses the same thermopile with a glass dome). Because $T_s$ is not directly measured, it must be calculated from $\Delta V$ and $T_c$ via (6) (see section 4a). Notice that we have made no assumptions that $\epsilon_o \approx 1.0$. In fact, $\epsilon_o$ does not appear in the equation except in the empirical calibration constant $s_o$.

The original values for $B$ given by Albrecht and Cox (1977) do not apply to modern silicon domes. A value of $B = 4.0$ can be found in World Meteorological Organization literature (e.g., Olivieri 1991). Miskolczi (1994) quotes a value of 4.4 but does not give a source. Philipona et al. (1995) give values ranging from 3.1 to 4.2 with an average of 3.58 based on five laboratory measurements of B. Foot (1997, personal communication), who used a value between 3.2 and 3.5 for the U.K. C-130 aircraft sensors based on measurement procedures at the U.K. Meteorological Office. Based on these values, for the purposes of this paper we will assume a nominal value of $B = 3.5$ with an rms uncertainty of about 0.5. A laboratory method to obtain $s_o$ and $B$ is described in Part II.

Expressions similar to (9) can be found in Alados-Arboledas et al. (1988), but their final derivation takes a different course because they emphasize corrections without measuring the dome temperature. Philipona et al. (1995) also rederive the radiometer equation, but they leave out one of the terms in $R_{\text{up}}$, so their analysis yields a coefficient in front of the $\sigma T_s^4$ term that is not identically 1.0. For the idealized situation of the analysis, this is incorrect (when $\tau$ is set to zero, their result violates a fundamental principle of thermodynamics that two objects in radiative thermal equilibrium must be at the same temperature regardless of their emissivities). Because the actual calibration relationship for the pyrgeometer may not be exactly described by the idealized derivation, Philipona et al. (1995) keep more empirical coefficients; these are determined by a complicated calibration procedure. Their calibrations of five radiometers indicate that the constant in front of the $\sigma T^4$ term is about 1.005.

## 3. Eppley calibration and interpretation

The calibration and interpretation of pyrgeometer data is a complex issue. One aspect of the problem is the technique used by Eppley to establish the thermopile output sensitivity constant. A second aspect is the method used to log the data, that is, which variables available from the instrument are actually measured and which of the various forms of the pyrgeometer equation are used. In this section we will discuss these issues. It is clear now that for those using only the calibration information supplied by Eppley, (11) is preferable to (7). If (7) is used, either in determining the calibration constants or in computing $H$ from the measurements, then errors are generated. We begin with an examination of the Eppley calibration method and then assess how this is interpreted in terms of the fundamental calibration equation.

### *a. The Eppley calibration method*

Eppley (1995) discussed the technique used to establish the calibration of each Eppley pyrgeometer in Eppley's Technical Procedure TP05, which we summarize here. A blackbody source consisting of a copper tank with an indented hemisphere painted with Parsons' Optical Black paint is filled with water and maintained by a temperature-controlled circulating bath. The pyrgeometer is raised into the hemisphere, and the thermopile voltage $\Delta V_B$, and case temperature $T_c$, are read after the instrument comes to equilibrium (after an exposure of roughly 1 min). This is done for blackbody source temperatures $T_B$ of approximately 5° and 15°C. The Eppley thermopile sensitivity is then computed as

$$s_e = \frac{\Delta V_B}{\sigma(T_B^4 - T_c^4)}, \tag{13}$$

and the final value for $s_e$ is obtained as an average from both temperatures. Note that the factor of $\epsilon_o$ does not appear (because, according to *TP05*, $\epsilon_o \approx 1$), and differences in dome and case temperature are ignored.

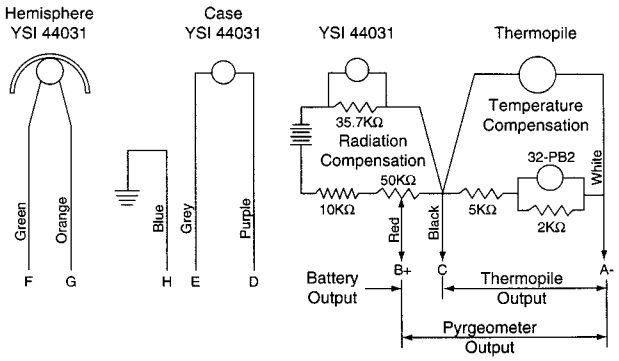


FIG. 2. Schematic of wiring and connections for the Eppley PIR.

For those interested in simplified data logging, Eppley included a battery-powered resistance network (see Fig. 2) to generate a voltage in series with the thermopile output that supplies the electrical equivalent to the second term in (7) with $\epsilon_o = 1$. The potentiometer is adjusted until the voltage output between terminals B and C, $\Delta V_{\text{bat}}$, is given by

$$\Delta V_{\text{bat}}/s_e = \sigma T_c^4. \tag{14}$$

Thus, a simple voltage measurement across terminals A and B, when multiplied by $s_e$, will yield the first two terms of (7). This process is described in the Instruction Sheet for the Eppley Precision Infrared Radiometer (Eppley Laboratory, Inc., 1994) available from the manufacturer, including instructions on checking the stability of the battery output and correcting its adjustment. The dome effect may be ignored, estimated with the solar flux parameterization of Alados-Arboledas et al. (1988), or determined explicitly by measurement of case and dome temperatures. Note that Eppley did not supply values for the empirical dome correction constant *B*.

### *b. Relationship to fundamental sensitivity*

We can use (11) to estimate the fundamental calibration constant, $s_o$, from the Eppley value. We express the blackbody source flux using (11):

$$(1 - \epsilon_c)\sigma T_R^4 + \epsilon_c \sigma T_B^4 = \Delta V_B/s_o + \sigma(T_c + \alpha \Delta V_B)^4 + B\sigma[(T_c + \alpha \Delta V)^4 - T_d^4], \tag{15}$$

where $T_R$ represents the blackbody temperature of the room, and the radiometer, and $\epsilon_c$ is the effective emissivity of the calibration source. Expanding the fourth-order sums, keeping only the first two terms, and rearranging, yields

$$(1 - \epsilon_c)\sigma(T_R^4 - T_B^4) + \sigma T_B^4 = \Delta V_B[1 + 4\alpha\sigma s_o T_c^3(1 + B)]/s_o + \sigma T_c^4 + B\sigma(T_c^4 - T_d^4). \tag{16}$$

However, we can also expand the rightmost term as the difference in the case and dome temperatures. Typical measurements show that in the absence of solar heating of the dome, this temperature difference is a fraction, $f$, of the case-thermopile difference,

$$(T_c^4 - T_d^4) \approx 4T_c^3(T_c - T_d) = -4T_c^3 f \Delta T = -4T_c^3 f \alpha \Delta V_B. \tag{17}$$

A linear regression (not shown) of $T_c - T_d$ versus $\Delta T$ for $\Delta T < -0.1$ K using data described in section 5a yielded a value of $f = 0.5$ with a correlation coefficient of 0.72 for 1069 1-min samples. We now solve for the thermopile output:

$$\Delta V_B = \frac{[(1 - \epsilon_c)\sigma(T_R^4 - T_B^4) + \sigma(T_B^4 - T_c^4)]}{\{1 + 4\alpha s_o \sigma[1 + B(1 - f)]T_c^3\}} s_o. \tag{18}$$

From (13) and (18) we compute $s_e$; we drop the $(1 - \epsilon_c)$ term because it appears multiplied by a flux *difference* [note that Albrecht et al. (1974) neglected a $(1 - \epsilon_o)$ term multiplied by a flux, which is two orders of magnitude larger than a flux difference] and solve for $s_o$:

$$s_o = s_e/\{1 - 4\alpha s_e \sigma[1 + B(1 - f)]T_c^3\}. \tag{19}$$

We can evaluate (19) using typical values and estimates of the calibration conditions: $T_c = 22°\text{C}$, $f = 0.5$, $B = 3.5$, and $s_e = 4.0\ \mu\text{V/(W m}^{-2})$. Thus, (19) yields $s_o/s_e = 1.043$, or the fundamental sensitivity constant of the pyrgeometer is about 4% greater than that determined by Eppley.

## 4. Accuracy evaluation

### *a. Error analysis*

To analyze the accuracy of the pyrgeometer, we begin by collecting the common terms from (11):

$$H = \Delta V/s_o + (1 + B)\sigma T_s^4 - B\sigma T_d^4. \tag{20}$$

Next, we use (6) to eliminate $T_s$ and express the equation in actual measured variables, expanding the fourth-order sum as before:

$$H = [1 + 4(1 + B)\sigma\alpha s_o T_c^3]\Delta V/s_o + (1 + B)\sigma T_c^4 - B\sigma T_d^4. \tag{21}$$

From our discussion at the end of section 3b, we note that the bracketed factor multiplying $\Delta V$ is approximately the same as in (19); thus, we replace $s_o$ with $s_e$ and represent $H$ as the sum of three terms:

$$H = \Delta V/s_e + (1 + B)\sigma T_c^4 - B\sigma T_d^4 = T_1 + T_2 + T_3. \tag{22}$$

We note that for typical measurement conditions near the surface, the downward IR flux will be primarily determined by the case temperature ($H \approx \sigma T_c^4 \approx \sigma T_d^4$), and the thermopile output term will be approximately equal to the net IR flux, ($H_{\text{net}} = H_{\text{dn}} - H_{\text{up}} \approx \Delta V/s_e$); thus,

TABLE 1. Sensitivity coefficients in $\mu$V/(W m$^{-2}$) of an ensemble of WHOI PIRs as determined by Eppley Laboratory's calibrations over the last eight years. The instruments are identified by serial number and the calibration by date.

| # | 7026 | 7238 | 7363 | 7927 | 7953 | 8379 | 8382 | 8458 | 8459 | 8461 | 8462 | 8872 |
|---|---|---|---|---|---|---|---|---|---|---|---|---|
| 6–88 | 4.14 | | | | | | | | | | | |
| 8–88 | | 4.22 | | | | | | | | | | |
| 11–88 | | | 3.61 | | | | | | | | | |
| 8–89 | 4.03 | 4.37 | | | | | | | | | | |
| 1–90 | | | | 3.45 | 3.45 | | | | | | | |
| 6–90 | | 4.42 | | | | | | | | | | |
| 12–90 | 3.99 | | 3.63 | | | | | | | | | |
| 2–91 | | | | | | 3.89 | 3.62 | | | | | |
| 3–91 | | | | | | | | 3.79 | 3.42 | 3.61 | | 3.70 |
| 6–91 | | 4.08 | | | | | | | | | 3.88 | |
| 11–91 | | | 3.53 | | | | | | | | | |
| 2–92 | | | 3.59 | | | | | | | | | |
| 5–92 | | | | 3.38 | 3.50 | | | | 3.27 | 3.45 | | 3.64 |
| 6–92 | 4.06 | | | | | | | 3.45 | | | | |
| 8–92 | | | | | | | 3.72 | | | | | |
| 3–93 | | | | | | 4.01 | 3.73 | | | | | |
| 4–93 | 4.36 | | | 3.44 | | | | | | | | |
| 5–93 | | 4.32 | | | | | | | | | | |
| 1–94 | | | | | | | | 3.65 | 3.22 | 3.43 | 3.45 | 4.02 |
| 5–94 | | 4.28 | | | | | | | 3.22 | | | |
| 8–94 | | | | | | 3.72 | | | | | 3.67 | |
| 12–94 | | | 3.50 | | | | | | | | | |
| 6–95 | | | | | 3.38 | | | | | | | |
| Number | 5 | 6 | 5 | 3 | 3 | 3 | 3 | 3 | 4 | 3 | 3 | 3 |
| $\langle s \rangle$ | 4.12 | 4.28 | 3.57 | 3.42 | 3.44 | 3.87 | 3.69 | 3.63 | 3.28 | 3.50 | 3.60 | 3.86 |
| $\sigma_s$ | 0.15 | 0.12 | 0.05 | 0.04 | 0.06 | 0.15 | 0.06 | 0.17 | 0.09 | 0.10 | 0.13 | 0.18 |
| $\sigma_s/\langle s \rangle$ (%) | 3.6 | 2.8 | 1.5 | 1.1 | 1.8 | 3.8 | 1.6 | 4.7 | 2.9 | 2.8 | 3.6 | 4.6 |

$$T_1 = H_{\text{net}}, \tag{23a}$$

$$T_2 = (1 + B)H, \tag{23b}$$

$$T_3 = -BH. \tag{23c}$$

When pointed at the sky the thermopile voltage is usually negative because the ''effective'' sky temperature is substantially less than the local ambient surface temperature. Finally, we take the first derivative of (22) and represent the normalized uncertainty of $H$ in terms of the various measurement uncertainties:

$$\delta H/H = \pm\frac{\delta(\Delta V)}{Hs_e} \pm \frac{H_{\text{net}}}{H}\frac{\delta s_e}{s_e} \pm 4(1 + B)\frac{\delta T_c}{T_c} \pm 4B\frac{\delta T_d}{T_d}. \tag{24}$$

The thermistors used to measure the temperatures are accurate to 0.1 K. We assume an additional 0.1 K uncertainty for $T_c$ and 0.2 K for $T_d$ because of temperature gradients in the system (see Philipona et al. 1995 for measurements of dome temperature at multiple locations), thus making the total uncertainty 0.15 K for $T_c$ and 0.22 K for $T_d$. We assume that we can average over AC line pickup and other sources of random noise, so the primary uncertainty in the thermopile voltage comes from residual thermoelectric voltages at wire junctions and biases in the voltage measurement system. It is difficult to reduce this uncertainty below 10 $\mu$V without taking special measures. Alados-Arboledas et al. (1988) suggested that the sensitivity constant is uncertain to 2.5%. However, a statistical analysis of an ensemble of calibrations of the Woods Hole Oceanographic Institution's (WHOI) PIR inventory taken over the last eight years (see Table 1) yields a standard deviation of 3.1%, which does not include any systematic errors in the Eppley procedure. We suggest that an uncertainty of 4% for the sensitivity constant would be more realistic. So, estimating the uncertainties in the variables as $\delta(\Delta V) \approx 10$ $\mu$V, $\delta s_e/s_e \approx 0.04$, $\delta T_c \approx 0.15$, $\delta T_d \approx 0.22$ K, and giving typical values for the net and downward IR fluxes, $H \approx 350 \pm 100$ W m$^{-2}$ and $H_{\text{net}} \approx -50 \pm 50$ W m$^{-2}$, we obtain

$$\delta H/H = \pm 0.007 \pm 0.006 \pm 0.009 \pm 0.009. \tag{25}$$

Assuming that these errors are uncorrelated, the total root-mean-square error is about 1.5% or 5 W m$^{-2}$. The 5 W m$^{-2}$ represent the absolute accuracy of the pyrgeometer as supplied by Eppley with the Eppley calibration constant, provided the thermopile output and both thermistors are recorded accurately and (11) or (22) is used to compute the flux. Except for modestly increasing the uncertainty of Eppley's determination of $s_e$ to 4% from our measurement of scatter of 3.1%, we have ignored any substantial bias in Eppley's calibrations; however, a doubling of the uncertainty of that term would only increase the total uncertainty to 1.8%.

Uncertainty in the $B$ coefficient adds to (25) a term $\delta B/B \times H_d/H$, where $H_d = B\sigma(T_c^4 - T_d^4)$. Averaged over a diurnal cycle, $H_d$ is on the order of 7 W m$^{-2}$ and $\delta B/$

$B$ is about $\pm 0.15$, so this term is about 0.003 (i.e., it does not significantly change the rms error). However, at noon $H_d$ can be as large as 30 W m$^{-2}$, so uncertainty in $B$ can increase the uncertainty in $H$ to 1.9%.

The least accurate approach is to use the battery-compensation output and ignore the dome effects. In this case the appropriate expression for $H$ is

$$H = (\Delta V + \text{constant } T_c^4)/s_e. \quad (26)$$

Performing the differential analysis as above yields

$$\delta H/H = \pm \frac{\delta(\Delta V)}{Hs_e} \pm \frac{\delta s_e}{s_e} \pm 4\frac{\delta T_c}{T_c} \pm \text{Dome}, \quad (27)$$

where we have added the uncertainty caused by omitting the dome contribution. Using the same measurement uncertainties, we find for this mode of operation,

$$\delta H/H = \pm 0.007 \pm 0.04 \pm 0.005 \begin{matrix} + 0.03 \\ - 0.00. \end{matrix} \quad (28)$$

Notice that the uncertainty in the sensitivity coefficient is now the largest source of error. This is because it is now applied not only to the thermopile output voltage but also to the battery-compensation voltage, which is nearly an order of magnitude larger. In other words, it is no longer an error in the *net* IR flux but an error in the *total downward* flux. In this case a doubling of the uncertainty in Eppley's determination of $s_e$ results in an uncertainty in the downward flux of 8%. Ignoring the dome effect causes negligible error at night, but during the day it is about 3.5% of the solar flux (Alados-Arboledas et al. 1988). These errors give a combined uncertainty on the order of 5% or 20 W m$^{-2}$. In (28) we have ignored the errors introduced by using the battery-resistance network to represent the case temperature contribution. For the temperature range 15°–30°C, this is only 1 W m$^{-2}$ (Albrecht and Cox 1977) but becomes substantially larger outside this range.

### b. Discussion

From the analysis presented above, we estimate that optimum recording and processing of the pyrgeometer information yields an absolute accuracy of about 5 W m$^{-2}$, but this degrades to at least 20 W m$^{-2}$ when using only the battery-compensated output. Ignoring the dome effect introduces a positive bias in the average downward IR flux of about 3.5% of the local diurnally averaged solar flux (roughly, $0.035 \times 200 = 7$ W m$^{-2}$) and introduces a diurnal cycle as large as 30 W m$^{-2}$. Use of the factor of $\epsilon_o = 0.98$ with the case temperature introduces a negative bias of $(1 - \epsilon_o)H$ or about $-7$ W m$^{-2}$. To the extent that the Eppley blackbody source accurately represents an IR flux standard, their calibration procedure produces an unbiased measurement of the absolute downward IR flux, even if the battery-compensation circuit is used. If we assume that variations in the sensitivity coefficient and at least part of the uncertainties in the temperature measurements have negligible variation on the 1-month timescale of a typical field program, then the instrument can provide significantly greater precision. Thus, field intercomparison against a more accurate secondary standard or correction to the average value of an ensemble of radiometers can translate this precision to improved absolute accuracy. Albrecht et al. (1974) and Philipona et al. (1995) both estimated this limit to be about 2.5 W m$^{-2}$. We have not attempted to analyze the effects of the bandpass of the silicon dome. Eppley Laboratory, Inc. (1976) described the lower wavelength limit as a sharp bandpass between 3 and 4 $\mu$m, but there have been reports that in some cases the cutoff is lower. Planck function calculations suggest that about 30 W m$^{-2}$ of solar flux falls above 2.8 $\mu$m, but because of atmospheric absorption and scattering and the transmission coefficient of the dome, Olivieri (1991) estimates this to be an error of only 1–2 W m$^{-2}$ at solar noon. Furthermore, contamination by solar flux in this manner is indistinguishable from dome heating and may explain the considerable variation in dome-heating coefficients observed between different radiometers (see Philipona et al. 1995 for a more detailed discussion).

## 5. Validation of fundamental equation

### a. Radiometer intercomparisons

In this section we examine two sets of side-by-side intercomparisons of PIRs to illustrate several of the points concerning accuracy, precision, and data methods. The first set of comparisons were postcalibrations of several PIRs used in the TOGA COARE–observing program. The units compared were the Environmental Technology Laboratory (ETL) radiometer from the R/V *Moana Wave*, the Commonwealth Scientific and Industrial Research Organization (CSIRO) radiometer from the R/V *Franklin*, and three WHOI radiometers. The units were mounted outdoors at the WHOI calibration site, and the data from all units were acquired with one processor system. The ETL and CSIRO units were set up to record both case and dome temperatures and the thermopile output; the WHOI units were set up to log only the battery-compensated output. A representative section of the time series of downward flux from the ETL and CSIRO units and two of the WHOI units is shown in Fig. 3. The two battery-compensated radiometers disagree by about 20 W m$^{-2}$, but the ETL and CSIRO units are much closer (the third WHOI unit fell in the middle of the group but is not shown in the graph to avoid further visual clutter). The larger scatter from the battery-compensated units is consistent with the discussion in section 4.

We focus attention on the ETL and CSIRO units. These were purchased at different times, both some years before this comparison, for which we use the original calibration provided by Eppley at the time of purchase. In Fig. 3 we can clearly see periods of close

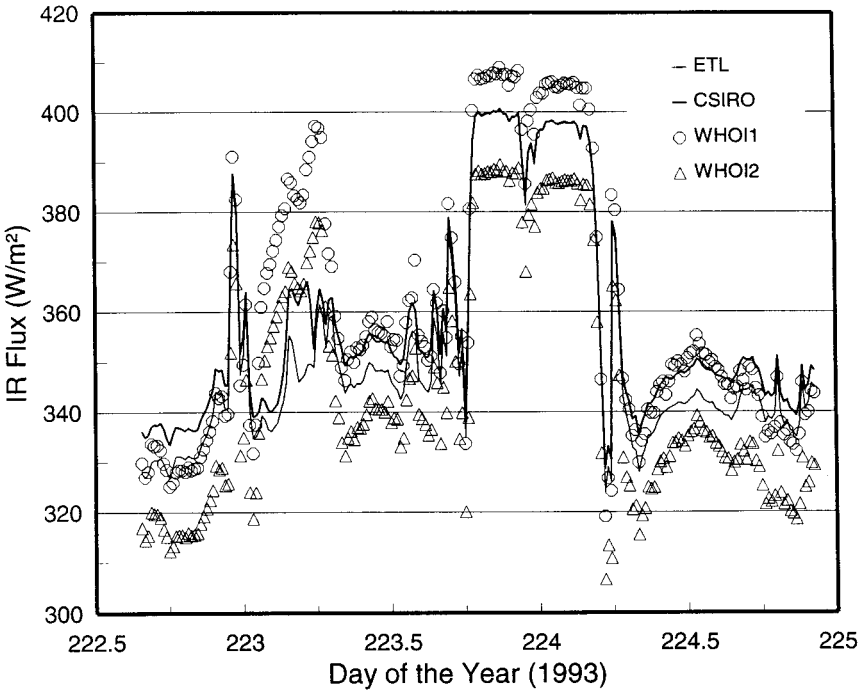


FIG. 3. Time series of PIR downwelling irradiance intercomparisons from the WHOI calibration period following TOGA COARE. The data designations are as follows: thin line, ETL radiometer; thick line, CSIRO radiometer; circle symbols, WHOI #1 radiometer; triangle symbols, WHOI #2 radiometer.

agreement and periods of disagreement by as much as 10 W $m^{-2}$. The nature of their disagreement is made clearer when we plot the difference in their values as a function of the thermopile output (Fig. 4a). The two radiometers agree closely when the thermopile output is small, and their disagreement increases linearly with thermopile output. Our conclusion is that the two units agree closely for the last two terms in (11) but differ in an amount proportional to the first term. We attribute this to inconsistencies in their thermopile-sensitivity coefficients. Without further calibration information to aid us, we adjusted the sensitivity coefficient of the CSIRO unit by 7% (i.e., the slope of the line in Fig. 4a) and recomputed the fluxes; the result is given in Fig. 4b. Now the mean relative offset of these instruments is less than 1 W $m^{-2}$, and their rms difference is less than 2 W $m^{-2}$. A comparison of the ETL and adjusted CSIRO flux time series (Fig. 5) now shows clear consistency. We have also used (22) to compute the flux from the ETL radiometer. The difference between flux computed using (22) and flux computed using (11) for this dataset has a mean of 0.9 W $m^{-2}$ and a standard deviation of 0.6 W $m^{-2}$ for 1069 10-min samples.

Now we compare two radiometers recently received from Eppley in a single shipment. These units were deployed for 27 days on the R/V *Discoverer* during a research cruise from Samoa to New Guinea to Hawaii. The units were mounted facing upward, side by side on a small mast at the aft end of the fantail. Again, both dome and case temperatures and thermopile outputs were recorded on a single datalogger. The difference between units is shown in Fig. 6a as a function of time and in Fig. 6b as a function of thermopile output. Note the absence of a clear linear trend in Fig. 6b, in contrast to Fig. 4a. Here, it is clear that the thermopile-sensitivity coefficients of these two units are quite consistent. However, the 5 W $m^{-2}$ diurnal cycle in the radiometer differences (Fig. 6a) indicates an inconsistency in the dome corrections for these two units. Again, we do not know what the actuality is, so we modified the dome correction factor $B$ from 2.5 to 3.0 on unit 1. This produced the results shown in Fig. 7. As in the previous case, there is a mean offset of the two units of about 1 W $m^{-2}$ and an rms difference of less than 2 W $m^{-2}$. Such adjustments can lead to improved net radiative flux measurements, but without some additional calibration they do not improve absolute accuracy. The difference between flux computed using (22) and flux computed using (11) for this dataset has a mean of 1.2 W $m^{-2}$ and a standard deviation of 1.1 W $m^{-2}$ for 3383 10-min samples.

### *b. Field comparisons with a Rapid Radiative Transfer Model (RRTM)*

In a clear atmosphere, the net longwave flux density at any height may be calculated from a temperature profile with knowledge of the thermal absorption and emission characteristics of the atmospheric gaseous con-

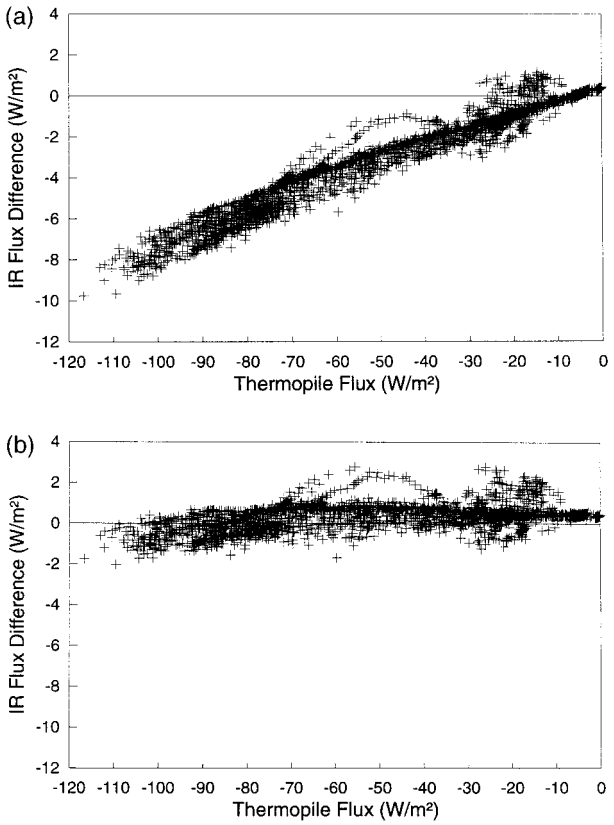


FIG. 4. The difference in the ETL and CSIRO IR irradiances vs the ETL thermopile output flux using (a) the factory calibration for the thermopile-sensitivity coefficient of the CSIRO instrument, $S_e$ = 4.26 $\mu$V/(W m$^{-2}$), and (b) the modified coefficient, $s_e$ = 3.97 $\mu$V/(W m$^{-2}$).

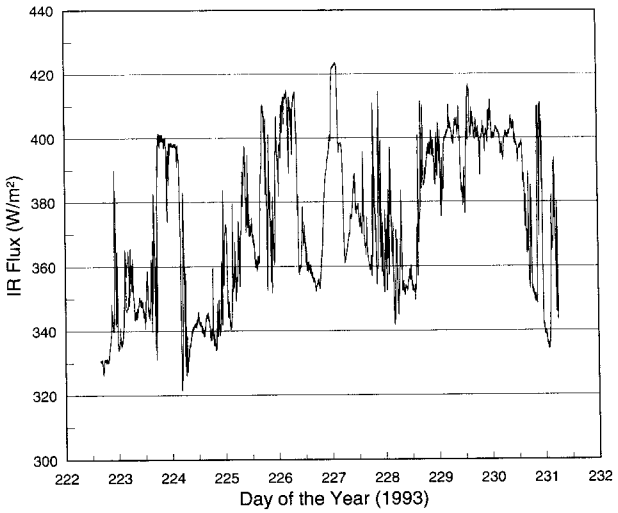


FIG. 5. As in Fig. 3 but for only the ETL radiometer and the CSIRO radiometer, using the modified thermopile-sensitivity coefficient for the entire intercomparison period.

stituents via an appropriate radiative transfer model (see, e.g., Paltridge and Platt 1976, chap. 7). Such models require as input the vertical concentration profiles of the atmospheric gases, the most important for infrared transfer being water vapor, carbon dioxide, and ozone. Global downwelling longwave radiation at the surface is thus obtained by integrating through the atmosphere. Over the years, many radiative transfer models have been developed, presumably increasing in sophistication in response to improved understanding and increased computer power. Such models have recently been used for direct comparison with PIR measurements (Miskolczi 1994). For example, Dutton (1993) showed an excellent comparison with a number of years of PIR data and the radiative transfer model LOWTRAN7. These data ranged from polar to tropical; regional mean differences were about $\pm 5$ W m$^{-2}$. The present study coincided with the release of version 2.0 of the RRTM developed for use by the Atmospheric Radiation Program (ARM) science team (Mlawer et al. 1997). E. Mlawer kindly provided us with his computer code, and we have used RRTM with COARE atmospheric soundings data to calculate downwelling longwave for comparison with the R/V *Moana Wave* pyrgeometer measurements.

RRTM presents the user with a wide number of input options that are fully described in the instructions provided; we used mostly the default options. The model allows for the use of up to 35 molecular species, defaulting to the seven most important: $H_2O$, $CO_2$, $O_3$, $N_2O$, CO, $CH_4$, and $O_2$. The user-defined atmospheric profile option requires successive lines containing altitude, pressure, and temperature, followed by as many species as are available in a choice of units. Of these molecular species, the COARE soundings contain only water vapor, for which we adopt the units of relative humidity since this is the primary measurement from the Väisälä sondes. An input file was written in the specified format from the sounding, using every reading to about 1-km altitude, then in 0.25-, 0.50-, 0.75-, 1.00-, and 5.00-km steps to 2.5-, 7-, 13-, 25-, and 50-km altitude, respectively, a possible 50 levels in all. The carbon dioxide surface concentration was set to 350 ppm, and, in the absence of direct profiles, it and the remaining five species were set to the tropical atmosphere profile available within RRTM, as was water vapor above the highest altitude of the sounding.

Six-hourly soundings were taken from a number of sites in the Intensive Flux Array (IFA) during COARE, and have been processed by the National Center for Atmospheric Research (NCAR) Surface and Soundings Systems Facility (Miller 1993). Many have required significant correction for near-surface temperature and humidity errors (Cole and Miller 1995), and the quality of the soundings data overall is still the subject of discussion (Bradley and Weller 1995; Bradley and Weller 1997). The obvious first choice for comparison with the R/V *Moana Wave* pyrgeometer are those soundings launched from R/V *Moana Wave* herself. However, at some stage during January 1993, the sounding humidities measured from the R/V *Moana Wave* were clearly

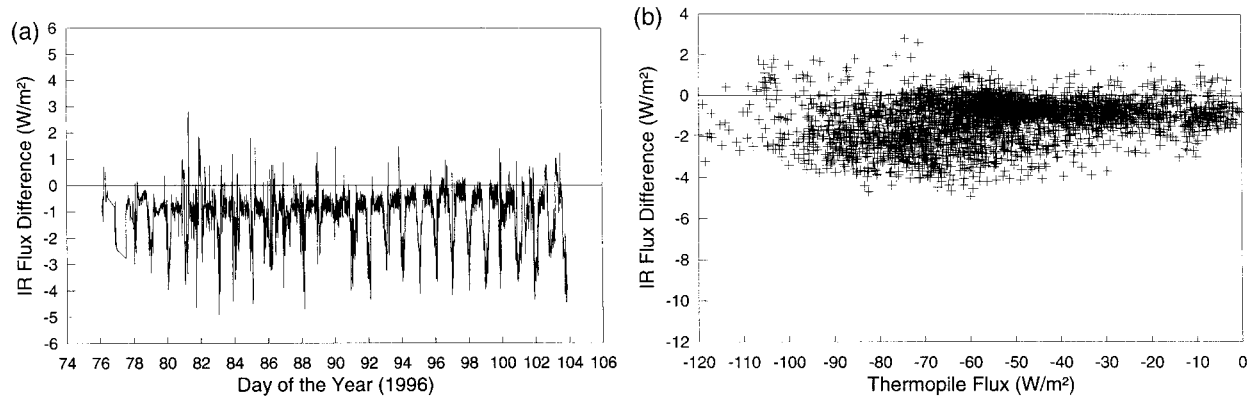


FIG. 6. Difference in measured downwelling irradiance between two PIRs mounted side by side vs (a) time and (b) thermopile output flux from one of the PIRs (unit 1).

too ''dry'' in the lower troposphere with a systematic bias of 0.5 g $kg^{-1}$, a problem ascribed to a batch of faulty sondes. Increasing the water vapor concentration of the entire sounding by 0.5 g $kg^{-1}$ increases the surface irradiance by 2 W $m^{-2}$, while increasing the lowest 1 km by 1.0 g $kg^{-1}$ increases the surface irradiance by 2.8 W $m^{-2}$. Of the remaining sites, there is agreement (R. Johnson and E. Zipser 1996, personal communication) that independent soundings taken on the R/V *Vickers* during leg 3 by the German group led by Dr. H. Grassl seem the most reliable. Fortunately, during the period when comparisons were possible, the R/V *Vickers* was operating within about 50 km of the R/V *Moana Wave*. Thus, all of the sondes used in this study are believed to be free of significant bias.

Absence of cloud is essential for valid application of radiative transfer models in general, although in the Tropics only the lowest 3 km of the atmospheric profile affects the surface longwave radiative flux (this is easily established with the model by artificially injecting blobs of water vapor at different heights and computing the surface irradiance). Thus, our results here are not subject to contamination by cirrus clouds, but that could be a problem at higher latitudes. Several sources of information were used to determine clear-sky conditions and thus to accept or reject a sounding for comparison. The Geostationary Meteorological Satellite (GMS) images and notes in the TOGA COARE Intensive Observing Period (IOP) Operations Summary (TCIPO 1993) were used to identify periods of generally settled weather. We also consulted the half-hourly photographs taken with all-sky cameras installed on R/V *Franklin* and R/V *Wecoma*; these ships were not necessarily close to the R/V *Moana Wave*, but even when distant gave some indication of overall conditions and the diurnal cloud pattern. The R/V *Moana Wave* rainfall record was helpful, and she also carried a ceilometer measuring cloud fraction and an indication of cloud-height distribution that, while needing some interpretation, complemented the visual methods.

Because of the sampling mismatch among the observations under comparison, periods of obvious atmospheric instability and convective activity were avoided. A sounding to 20 km typically takes 1.5 h to complete. The R/V *Moana Wave* pyrgeometer and ceilometer data used for comparison was the hourly average following the sonde launch (nominally at 0000, 0600, 1200, and 1800 UTC). Three periods of a few days each

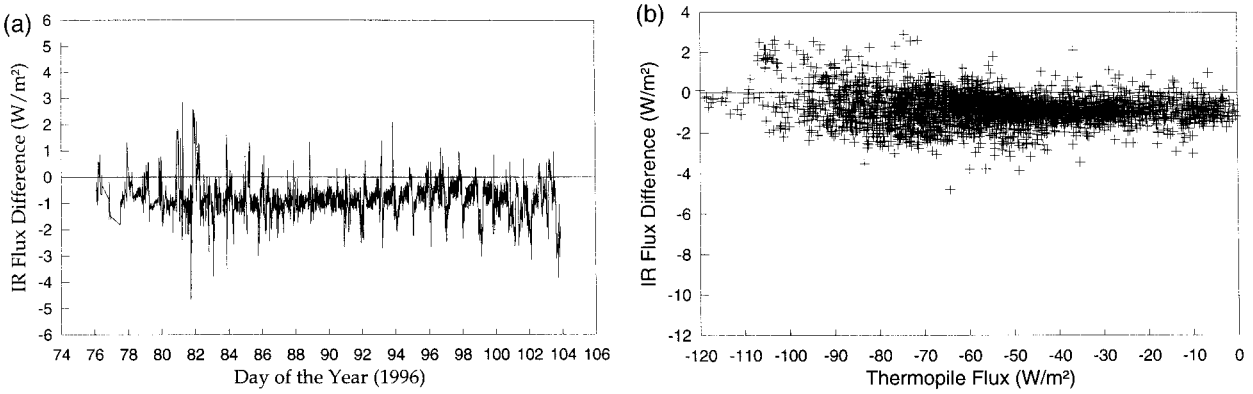


FIG. 7. As in Fig. 6 but after changing the dome-heating coefficient *B* from 2.5 to 3.0 for unit 1.

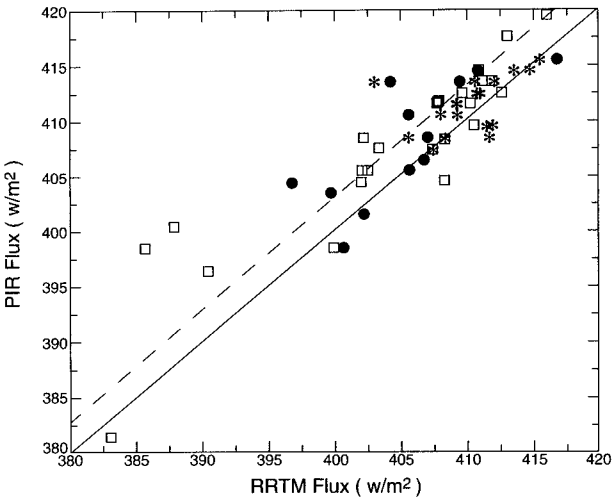


FIG. 8. Scatter diagram of R/V *Moana Wave* PIR downwelling flux vs flux computed from RRTM using radiosonde temperature and humidity profiles obtained in cloud-free conditions. The different symbols denote the sampling periods: triangles, 12–23 November 1992; stars, 27 November–3 December 1992; circles, 1–5 February 1993. The solid line is a perfect 1:1 fit; the dashed line is offset by 2.1 W $m^{-2}$.

were selected during which a large fraction of soundings seemed unaffected by cloud.

- 12–23 November 1992. From a total of 39 soundings launched from the R/V *Moana Wave* during this period, 14 were not used because of cloud.
- 27 November–3 December 1992. Of the 22 R/V *Moana Wave* soundings during this period, only 4 were launched in cloudy conditions. This period included the first multiship and aircraft intercomparison on 28 November (Bradley et al. 1996, manuscript submitted to *J. Atmos. Oceanic Technol.*).
- 2–5 February 1993. This was an unbroken series of 12 soundings launched from the R/V *Vickers* in cloud-free conditions. It included the second multiship intercomparison on 4 February.

Using the pyrgeometer equation (11) developed here for the analysis of R/V *Moana Wave* PIR data during COARE rather than the Albrecht–Eppley equation (7) results in an average increase in downwelling longwave radiation of 9.4 W $m^{-2}$. Figure 8 shows the PIR hourly measurements computed with (11), compared with the RRTM downwelling longwave output at the surface, for the three periods specified above. The mean difference between the sets of data is 2.1 W $m^{-2}$, as indicated by the broken line; that is, the radiative transfer model supports the use of (11) rather than (7) but indicates that the correction should be slightly less, around 7.3 W $m^{-2}$. The standard deviation of the data points about the dashed line in Fig. 8 is 3.5 W $m^{-2}$. Separate day–night comparisons (not shown) gave the same results.

Regarding the accuracy of RRTM, Mlawer advises that Atmospheric and Environmental Research, Inc. (AER), validates this model against their line-by-line radiative transfer model (LBLRTM) and rely on LBLRTM validations against measurement. They have not seen any longwave validation in which RRTM and LBLRTM differ by as much as 1.0 W $m^{-2}$ at any altitude, and, based on a large number of validations with well-specified water-vapor profiles, LBLRTM has a demonstrated (Mlawer et al. 1997) accuracy of 2 W $m^{-2}$. This is well within the accuracy goal for COARE flux measurements, so that the reliability of the present comparisons depends entirely on the accuracy of the COARE humidity soundings. As noted above, the R/V *Vickers* soundings are regarded as the most reliable, on the basis of analyses of atmospheric mixed-layer structures and calculations of convective available potential energy (CAPE).

Two series of side-by-side field intercomparisons conducted during COARE offer us an opportunity to evaluate the output of an ensemble of PIRs relative to RRTM. We use the *Moana Wave*'s known relationship with RRTM to reference the readings of five other radiometers on four other platforms (Bradley and Weller 1997; Bradley et al. 1996, manuscript submitted to *J. Atmos. Oceanic Technol.*) for the intercomparison periods. The *Moana Wave* radiometer was logged optimally (i.e., thermopile voltage, case temperature, and dome temperature were recorded), while the others were logged in various suboptimal combinations. Each radiometer has been corrected for dome heating using either (11) or Alados-Arboledas et al. (1988); factory calibration coefficients were used. The following corrections in watts per square meter must be added to the individual radiometer's flux values to make them agree, on average, with RRTM: R/V *Franklin*, 0; R/V *Moana Wave*, −2; buoy IMET1, −5; buoy IMET2, +5; R/V *Hakuho*, +1; R/V *Wecoma*, +7. This ensemble of corrections exhibits a mean bias of 1.0 W $m^{-2}$ and an rms of 4.6 W $m^{-2}$. Thus, a *particular* unit from our modest collection of Eppley PIRs is characterized by a point-to-point scatter of about 4 W $m^{-2}$ (i.e., the scatter shown in Fig. 8) riding on top of a bias on the order of 5 W $m^{-2}$ (i.e., the scatter in individual biases from the six-radiometer ensemble), although we have little information on the temporal reproducibility of the bias. Taking RRTM to represent the correct clear-sky downwelling longwave flux, this limited analysis reveals no significant mean bias in the Eppley calibration procedure (i.e., the mean bias of our PIR ensemble was only 1 W $m^{-2}$).

### c. Applications to geophysical data

In this section we examine an application of PIRs to the simple problem of deducing the surface temperature from coincident upward and downward flux measurements. Surface temperature is a good test because it is usually measurable to an accuracy of a few tenths of a kelvin, while 1 K corresponds to an IR flux of about 5

W m $^{-2}$. This example illustrates the importance of the proper calibration equation and the accuracy of the units when optimally utilized.

To illustrate the impact of using (11) rather than (7), we use a comparison of in situ measurements of sea surface temperature from R/P *FLIP* with simultaneous values deduced from coincident measurements of upward and downward longwave flux using the same pair of Eppley PIRs as were used on the R/V *Discoverer* cruise discussed in section 5a. *FLIP* was moored 20 km off the Oregon coast for a period of three weeks in September and October 1995. Upward- and downward-facing PIRs and Eppley pyranometers were mounted on a 1-m-long strut near the end of *FLIP*'s face boom. The radiometers were 16 m from *FLIP*'s superstructure, which is about 20 m tall. The strut was placed normal to the boom with only a small rope handrail in the upward-facing radiometer's field of view. The data were logged as described previously. A floating thermistor was used to measure the bulk ocean water temperature at a depth of about 5 cm. The interfacial temperature was computed from this bulk measurement using the cool-skin algorithm of Fairall et al. (1996b) with an accuracy estimated to be $\pm 0.1$ K (Fairall et al. 1996a). The interfacial surface water temperature was computed from the PIR measurements using

$$T_s = \left[\frac{H_{\rm up} - (1 - \epsilon_s)H_{\rm dn}}{\epsilon_s \sigma}\right]^{1/4}, \qquad (29)$$

where $\epsilon_s$ is the emissivity of seawater that is assumed to be 0.97 (Fairall et al. 1996a). No correction was made for reflection of the thermal image of *FLIP*'s boom. Two different values of radiative temperature were computed: one with (7) and $\epsilon_o = 0.98$, and a second with (11). The results for a portion of the total time series are given in Fig. 9. The values obtained using (7) are clearly much too low. The mean difference between the in situ value and the correct radiative value caused by the cool-skin effect is 0.25 K, representing a difference in IR flux of about 1.5 W m$^{-2}$.

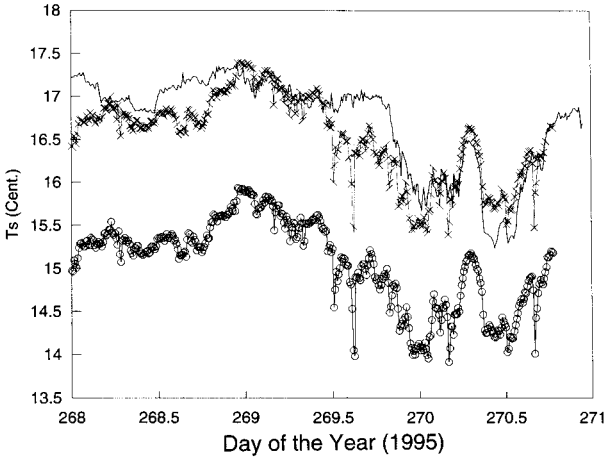


FIG. 9. Sea surface temperature vs time from a short period of measurements from R/P *FLIP* off the Oregon coast. The solid line is from direct in situ measurements with a floating thermistor in the upper 5 cm of the water, corrected to skin sea surface temperature using cool-skin theory (Fairall et al. 1996b). The crosses are computed using (29) from simultaneous measurements of upwelling and downwelling longwave irradiance with a pair of pyrgeometers. The longwave irradiances were computed using (11). The circles are similar to the crosses, except longwave irradiance was computed using (7) with $\epsilon_o = 0.98$.

## 6. Conclusions

In this paper we present a fundamental reexamination of the pyrgeometer and its application to the measurement of terrestrial radiation. A rigorous derivation of the heat balance equation for the pyrgeometer showed that a calibration equation in common use in the geophysical community contains an erroneous factor for the emissivity of the thermopile multiplying the $\sigma T^4$ term that represents most of the flux computed from the instrument. Use of a realistic value for emissivity causes an underestimate of the flux of 5–10 W m$^{-2}$, which is a very significant error in some geophysical applications. It has implications for the accuracy of radiatively derived surface temperature, bulk estimates of the surface sensible and latent heat fluxes, and the crucial net heat exchange between atmosphere and ocean. We also derived a more fundamental form of the calibration equation where the thermopile-sensitivity coefficient is independent of temperature (except for possible inadequacies in the thermopile temperature compensation built in by the manufacturer), and we showed that this coefficient is about 4% larger than that obtained using the old equation with the Eppley calibration procedures. However, use of the old equation with $\epsilon_o$ set to 1.0 gives results within 1–2 W m$^{-2}$ of the new equation if local conditions are reasonably close to the ambient conditions during the Eppley calibration process. A complete error analysis showed that the PIR has a basic precision of 1.5% of the total radiative flux, or about 5 W m$^{-2}$, when the thermopile voltage and both dome and case temperatures are measured independently. Logging only the battery-compensated thermopile output leads to errors in the total flux of about 5% or 20 W m$^{-2}$.

Several experimental aspects of the absolute and relative accuracy of the PIR were also examined. Using a database of 55 conventional radiosonde profiles of temperature and humidity obtained in cloud-free conditions during the TOGA COARE program, we compared measurements of downward IR flux from the R/V *Moana Wave* PIR with values computed with a community radiative transfer model called RRTM (Mlawer et al. 1997). The model and measurements were well correlated with a mean offset of 2.1 W m$^{-2}$ and an rms scatter about the offset line of 3.5 W m$^{-2}$. Steady improvements in radiosonde humidity and temperature measurement, and in the accuracy and speed of radiative transfer models, indicate that clear-sky model flux computations

might now take the role of a secondary absolute field standard against which to compare the PIR and to realize its full precision (see also Dutton 1993; Miskolczi 1994). To significantly reduce the PIR bias, the average humidity bias of the sondes used must be less than about 2% and care must be taken to ensure that there are no radiatively relevant clouds in the field of view.

Two different sets of side-by-side intercomparisons of PIRs were used to illustrate ways to detect calibration factor inconsistencies between radiometers. In one case, inconsistencies in thermopile-sensitivity coefficients $s_e$ were revealed by plotting the difference in radiometer fluxes versus the thermopile output. In the second case, we examined fluxes from two PIRs computed assuming identical values for the dome heating coefficient *B.* An observed diurnal variation of the difference in fluxes between the radiometers was reduced by a simple adjustment of the value of *B* for one unit. After these simple adjustments, the radiometer pairs agreed within 1 W $m^{-2}$ mean and 2 W $m^{-2}$ rms. Of course, a secondary standard is required to reconcile these differences in an absolute sense.

Finally, we used data from a field program in which pairs of PIRs were operated to measure both upwelling and downwelling IR flux simultaneously. These data were used to estimate the surface temperature over the ocean. Using independent estimates of the surface temperature, we showed that the old, erroneous calibration equation led to underestimates of the surface temperature between 1 and 2 K, while the new equation was within a few tenths of a kelvin.

*Acknowledgments.* This work is supported by the NOAA Climate and Global Change Program, the Department of Energy Atmospheric Radiation Measurement Program, and the CSIRO Climate Change Research Program. We thank Eli Mlawer for providing us with the RRTM code and John Bryan, who implemented it with the COARE soundings. The comments of three anonymous reviewers were helpful in improving the manuscript.

## REFERENCES

Alados-Arboledas, L., J. Vida, and J. I. Jiménez, 1988: Effects of solar radiation on the performance of pyrgeometers with silicon domes. *J. Atmos. Oceanic Technol.,* **5,** 666–670.

Albrecht, B. A., and S. K. Cox, 1977: Procedures for improving pyrgeometer performance. *J. Appl. Meteor.,* **16,** 188–197.

——, M. Poellot, and S. K. Cox, 1974: Pyrgeometer measurements from aircraft. *Rev. Sci. Instrum.,* **45,** 33–38.

Bradley, E. F., and R. A. Weller, Eds., 1993: Report on the First COARE Flux Working Group Meeting. Report, TCIPO, Boulder, CO, 20 pp. [Available from TOGA COARE International Project Office, University Corporation for Atmospheric Research, P.O. Box 3000, Boulder, CO 80307-3000.]

——, and ——, Eds., 1995: Joint Workshop of the TOGA COARE Flux and Atmospheric Working Groups. Report, TCIPO, Boulder, CO, 35 pp. [Available from TOGA COARE International Project Office, University Corporation for Atmospheric Research, P.O. Box 3000, Boulder, CO 80307-3000.]

——, and ——, Eds., 1997: Fourth Workshop of the TOGA COARE Air–Sea Interaction (Flux) Working Group. Report, TCIPO, Boulder, CO, 61 pp. [Available from TOGA COARE International Project Office, University Corporation for Atmospheric Research, P.O. Box 3000, Boulder, CO 80307-3000.]

Cole, H. L., and E. R. Miller, 1995: A correction for low-level radiosonde temperature and humidity measurements. *Proc. Ninth Symp. on Meteorological Observations and Instrumentation,* Charlotte, NC, Amer. Meteor. Soc., 32–36.

Dutton, E. G., 1993: An extended comparison between LOWTRAN-7 computed and observed broadband thermal irradiance: Global extreme and intermediate surface conditions. *J. Atmos. Oceanic Technol.,* **10,** 326–336.

Enz, J. W., J. C. Klink, and D. G. Baker, 1975: Solar radiation effects on pyrgeometer performance. *J. Appl. Meteor.,* **14,** 1297–1302.

Eppley Laboratory, Inc., 1976: Instrumentation for the measurement of the components of solar and terrestrial radiation. Eppley Laboratory, Newport, RI, 16 pp. [Available from Eppley Laboratories, P.O. Box 419, Newport, RI 02840.]

——, 1994: Instruction sheet for the Eppley precision infrared radiometer (PIR). Eppley Laboratory, Newport, RI, 5 pp. [Available from Eppley Laboratories, P.O. Box 419, Newport, RI 02840.]

——, 1995: Blackbody calibration of the precision infrared radiometer, model PIR. Tech. Procedure 05, Eppley Laboratory, Newport, RI, 1 p. [Available from Eppley Laboratories, P.O. Box 419, Newport, RI 02840.]

Fairall, C. W., J. E. Hare, and J. B. Snider, 1990: An eight-month sample of marine stratocumulus cloud fraction, albedo, and integrated liquid water. *J. Climate,* **3,** 847–864.

——, E. F. Bradley, D. P. Rogers, J. B. Edson, and G. S. Young, 1996a: Bulk parameterization of air–sea fluxes for Tropical Ocean-Global Atmosphere Coupled Ocean–Atmosphere Response Experiment. *J. Geophys. Res.,* **101,** 3747–3764.

——, ——, J. S. Godfrey, G. A. Wick, J. B. Edson, and G. S. Young, 1996b: Cool-skin and warm-layer effects on sea surface temperature. *J. Geophys. Res.,* **101,** 1295–1308.

Fritschen, L. J., and L. W. Gay, 1979: *Environmental Instrumentation.* Springer-Verlag, 216 pp.

Katsaros, K. B., and J. E. DeVault, 1986: On irradiance measurement errors at sea due to tilt of pyranometers. *J. Atmos. Oceanic Technol.,* **3,** 740–745.

MacWhorter, M. A., and R. A. Weller, 1991: Error in measurements of incoming shortwave radiation made from ships and buoys. *J. Atmos. Oceanic Technol.,* **8,** 108–117.

Miller, E., 1993: TOGA COARE Integrated Sounding System data report. Vol. 1, Surface and sounding data. NCAR and TCIPO, Boulder, CO, 67 pp. [Available from TOGA COARE International Project Office, University Corporation for Atmospheric Research, P.O. Box 3000, Boulder, CO 80307-3000.]

Miskolczi, F., 1994: Modeling of downward surface longwave flux density for global change applications and comparison with pyrgeometer measurements. *J. Atmos. Oceanic Technol.,* **11,** 608–612.

——, T. O. Aro, M. Iziomon, and R. T. Pinker, 1997: Surface radiative fluxes in sub-Sahel Africa. *J. Appl. Meteor.,* **36,** 521–530.

Mlawer, E. J., S. J. Taubman, P. D. Brown, M. J. Iacono, and S. A. Clough, 1997: Radiative transfer for inhomogeneous atmospheres: RRTM, a validated correlated-k model for the longwave. *J. Geophys. Res.,* **102,** 16 663–16 682.

Olivieri, J., 1991: Measurement of longwave downward irradiance using a PIR pyrgeometer. WMO Tech. Document, WMO/TD 453, 26 pp.

Paltridge, G. W., and C. M. R. Platt, 1976: *Radiative Processes in Meteorology and Climatology.* Elsevier, 318 pp.

Payne, R. E., and S. P. Anderson, 1999: A new look at calibration and use of Eppley precision infrared radiometers: Part II.

Calibration and use of the WHOI IMET PIR. *J. Atmos. Oceanic Technol.*, in press.
Philipona, R., C. Frohlich, and C. Betz, 1995: Characterization of pyrgeometers and the accuracy of atmospheric long-wave radiation measurements. *Appl. Opt.*, **34,** 1598–1605.
Ruffieux, D., P. O. G. Persson, C. W. Fairall, and D. E. Wolfe, 1995: Ice pack and lead surface energy budgets during LEADEX 1992. *J. Geophys. Res.*, **100,** 4593–4612.
TCIPO, 1993: TOGA COARE intensive observing period operations summary. Report, TCIPO, Boulder, CO, 492 pp. [Available from TOGA COARE International Project Office, University Corporation for Atmospheric Research, P.O. Box 3000, Boulder, CO 80307-3000.]
Webster, P. J., and R. Lukas, 1992: TOGA COARE: The Coupled Ocean–Atmosphere Response Experiment. *Bull. Amer. Meteor. Soc.*, **73,** 1377–1416.
Weiss, A., 1981: On the performance of pyrgeometers with silicon domes. *J. Appl. Meteor.*, **20,** 962–965.